



EUROPEAN ORGANIZATION FOR NUCLEAR RESEARCH

CERN-PPE/91-194

11 November 1991

Multiplicity Dependence of Mean Transverse Momentum in e^+e^- Annihilations at LEP Energies

DELPHI Collaboration

Abstract

A strong increase of the mean transverse momentum $\langle p_t \rangle$ with the number of charged particles n_{ch} is observed in e^+e^- annihilations into hadrons at LEP energies. The effect resembles correlations observed in hadron - hadron interactions. In e^+e^- annihilations the $\langle p_t \rangle$ and n_{ch} correlations can be accounted for by gluon radiation.

(Submitted to Physics Letters B)

P.Abreu¹⁸, W.Adam⁴³, F.Adami³⁴, T.Adye³², T.Akesson²¹, G.D.Alekseev¹³, P.Allen¹², S.Almehed²¹,
 S.J.Alvsvaag⁴, U.Amaldi⁷, E.Anassontzis³, P.Antilogus²², W.D.Apel¹⁴, R.J.Apsimon³², B.Åsman³⁸, P.Astier²⁰,
 J-E.Augustin¹⁶, A.Augustinus²⁷, P.Baillon⁷, P.Bambade¹⁶, F.Barao¹⁸, R.Barate¹¹, G.Barbiellini⁴⁰,
 D.Y.Bardin¹³, A.Baroncelli³⁵, O.Barring²¹, W.Bartl⁴³, M.J.Bates³⁰, M.Battaglia²⁸, M.Baubillier²⁰,
 K-H.Becks⁴⁵, C.J.Beeston³⁰, M.Begalli¹⁰, P.Beilliere⁶, Yu.Belokopytov³⁷, K.Belous³⁷, P.Beltran⁹, D.Benedic⁶,
 J.M.Benloch⁴², M.Berggren¹⁶, D.Bertrand², F.Bianchi³⁹, M.S.Bilenky¹³, P.Billoir²⁰, J.Bjarne²¹, D.Bloch⁶,
 S.Blyth³⁰, V.Bocci³³, P.N.Bogolubov¹³, T.Bolognese³⁴, M.Bonapart²⁷, M.Bonesini²⁵, W.Bonivento²⁵,
 P.S.L.Booth¹⁹, M.Boratav²⁰, P.Borgeaud³⁴, G.Borisov³⁷, H.Borner⁷, C.Bosio³⁵, B.Bostjancic⁷, O.Botner⁴¹,
 B.Bouquet¹⁶, C.Bourdarios¹⁶, M.Bozzo¹⁰, S.Braibant², P.Branchini³⁵, K.D.Brand³¹, R.A.Brenner¹²,
 C.Bricman², R.C.A.Brown⁷, N.Brummer²⁷, J-M.Brunet⁶, L.Bugge²⁹, T.Buran²⁹, H.Burmeister⁷,
 J.A.M.A.Buytaert⁷, M.Caccia⁷, M.Calvi²⁵, A.J.Camacho Rozas³⁶, A.Campion¹⁹, T.Camporesi⁷, V.Canale³³,
 F.Cao², F.Carena⁷, L.Carroll¹⁹, C.Caso¹⁰, E.Castelli⁴⁰, M.V.Castillo Gimenez⁴², A.Cattai⁷, F.R.Cavallo⁵,
 L.Cerrito³³, A.Chan¹, P.Charpentier⁷, L.Chaussard¹⁶, P.Checchia³¹, G.A.Chelkov¹³, L.Chevalier³⁴,
 P.Chliapnikov³⁷, V.Chorowicz²⁰, R.Cirio³⁹, M.P.Clara³⁹, P.Collins³⁰, J.L.Contreras²³, R.Contri¹⁰, G.Cosme¹⁶,
 F.Couchot¹⁶, H.B.Crawley¹, D.Crennell³², G.Crosetti¹⁰, M.Crozon⁶, J.Cuevas Maestro³⁸, S.Czellar¹²,
 S.Dagoret¹⁶, E.Dahl-Jensen²⁶, B.Dalmagne¹⁶, M.Dam²⁹, G.Damgaard²⁶, G.Darbo¹⁰, E.Daubie²,
 P.D.Dauncey³⁰, M.Davenport⁷, P.David²⁰, C.Defoix⁶, D.Delikaris⁷, S.Delorme⁷, P.Delpierre⁶, N.Demaris³⁹,
 A.De Angelis⁴⁰, M.De Beer³⁴, H.De Boeck², W.De Boer¹⁴, C.De Clercq², M.D.M.De Fes Laso⁴², N.De Groot²⁷,
 C.De La Vaissiere²⁰, B.De Lotto⁴⁰, A.De Min²⁵, H.Dijkstra⁷, L.Di Ciaccio³³, F.Djama⁸, J.Dolbeau⁹, O.Doll⁴⁵,
 M.Donsselmann²⁷, K.Doroba⁴⁴, M.Dracos⁷, J.Drees⁴⁵, M.Dris²⁸, Y.Dufour⁶, W.Dulinski⁸, L-O.Eek⁴¹,
 P.A.-M.Eerola⁷, T.Ekelof⁴¹, G.Ekspong³⁸, A.Elliot Peisert³¹, J-P.Engel⁸, D.Fassouliotis²⁸, M.Feindt⁷,
 M.Fernandes Alonso³⁶, A.Ferrer⁴², T.A.Filippas²⁸, A.Firestone¹, H.Foeth⁷, E.Fokitis²⁸, P.Folegati⁴⁰,
 F.Fontanelli¹⁰, K.A.J.Forbes¹⁹, H.Forsbach⁴⁵, B.Franek³², P.Frenkiel⁶, D.C.Fries¹⁴, A.G.Frodesen⁴,
 R.Fruhworth⁴³, F.Fulda-Quenser¹⁶, K.Furnival¹⁹, H.Furstenau¹⁴, J.Fuster⁷, G.Galeazzi³¹, D.Gamba³⁹,
 C.Garcia⁴², J.Garcia³⁶, C.Gaspar⁷, U.Gasparini³¹, P.Gavillet⁷, E.N.Gasis²⁸, J-P.Gerber⁸, P.Giacomelli⁷,
 K-W.Glitsa⁴⁵, R.Gokieli⁷, V.M.Golovatyuk¹³, J.J.Gomez Y Cadenas⁷, A.Goobar³⁸, G.Gopal³², M.Gorski⁴⁴,
 V.Gracco¹⁰, A.Grant⁷, F.Grand², E.Graziani³⁵, G.Grosdidier¹⁶, E.Gross⁷, P.Grosse-Wiesmann⁷, B.Grossetete²⁰,
 J.Guy³², F.Hahn⁷, M.Hahn¹⁴, S.Haider²⁷, Z.Hajduk¹⁵, A.Hakansson²¹, A.Hallgren⁴¹, K.Hamacher⁴⁵,
 G.Hamel De Monchenault³⁴, F.J.Harris³⁰, B.W.Heck⁷, T.Henkes⁷, I.Herbst⁴⁵, J.J.Hernandez⁴², P.Herquet²,
 H.Herr⁷, I.Hietanen¹², C.O.Higgins¹⁹, E.Higon⁴², H.J.Hilke⁷, S.D.Hodgson³⁰, T.Hofmokl⁴⁴, R.Holmes¹,
 S.O.Holmgren³⁸, D.Holthuisen²⁷, P.F.Honore⁶, J.E.Hooper²⁶, M.Houlden¹⁹, J.Hrubic⁴³, P.O.Hulth³⁸,
 K.Hultqvist³⁸, D.Husson⁸, P.Ioannou³, D.Isenhower⁷, P-S.Iversen⁴, J.N.Jackson¹⁹, P.Jalocha¹⁵, G.Jarlskog²¹,
 P.Jarry³⁴, B.Jean-Marie¹⁶, E.K.Johansson³⁸, D.Johnson¹⁹, M.Jonker⁷, L.Jonsson²¹, P.Juillot⁸, G.Kalkanis⁷,
 G.Kalmus³², F.Kapusta²⁰, A.Katargin³⁷, S.Katsanevas³, E.C.Katsoufis²⁸, R.Keranen¹², J.Kesteman²,
 B.A.Khomenko¹³, N.N.Khovanski¹³, B.King¹⁹, N.J.Kjaer⁷, H.Klein⁷, W.Klempt⁷, A.Klovning⁴, P.Kluit²⁷,
 A.Koch-Mehrin⁴⁵, J.H.Koehne¹⁴, B.Koene²⁷, P.Kokkinias⁹, M.Kopf¹⁴, M.Koratzinos³⁹, K.Korcyl¹⁵,
 A.V.Korytov¹³, V.Kostiukhin³⁷, C.Kourkournelis³, T.Kreuzberger⁴³, J.Krolikowski⁴⁴, I.Kronkvist²¹, J.Krstic³⁰,
 U.Kruener-Marquis⁴⁵, W.Krupinski¹⁵, W.Kucewicz²⁵, K.Kurvinen¹², C.Lacasta⁴², C.Lambropoulos⁹,
 J.W.Lamsa¹, L.Lanceri⁴⁰, V.Lapin³⁷, J-P.Laugier³⁴, R.Lauhakangas¹², G.Leder⁴³, F.Ledroit¹¹, R.Leitner⁷,
 Y.Lemoigne³⁴, J.Lemonne², G.Lenzen⁴⁵, V.Lepeltier¹⁶, A.Letessier-Selvon²⁰, E.Lieb⁴⁵, D.Liko⁴³, E.Lillethun⁴,
 J.Lindgren¹², A.Lipniacka⁴⁴, I.Lippi³¹, R.Llosa²³, B.Loerstad²¹, M.Lokajicek¹³, J.G.Loken³⁰,
 A.Lopes-Fernandes¹⁶, M.A.Lopes Agueras³⁶, M.Los²⁷, D.Loukas⁹, A.Lounis⁸, J.J.Lozano⁴², P.Luts⁶, L.Lyons³⁰,
 G.Machlum⁷, N.Magnussen⁴⁵, J.Maillard⁶, A.Maltezos⁹, F.Mandi⁴³, J.Marco³⁶, M.Margoni³¹, J-C.Marin⁷,
 A.Markou⁹, S.Marti⁴², L.Mathis¹, F.Matorras³⁶, C.Matteuzzi²⁵, G.Matthiae³³, M.Massucato³¹,
 M.Mc Cubbin¹⁹, R.Mc Kay¹, R.Mc Nulty¹⁹, E.Menichetti³⁹, G.Meola¹⁰, C.Meroni²⁵, W.T.Meyer¹,
 M.Michelotto³¹, W.A.Mitaroff⁴³, G.V.Mitselmakher¹³, U.Mjoernmark²¹, T.Moa³⁸, R.Moeller²⁸, K.Moenig⁷,
 M.R.Monge¹⁰, P.Morettini¹⁰, H.Mueller¹⁴, W.J.Murray³², B.Muryn¹⁶, G.Myatt³⁰, F.Naraghi²⁰,
 U.Nau-Korzen⁴⁵, F.L.Navarria⁵, P.Negri²⁵, B.S.Nielsen²⁶, B.Nijjar¹⁹, V.Nikolaenko³⁷, V.Obrastsov³⁷,
 K.Oesterberg¹², A.G.Olshevski¹³, R.Orava¹², A.Ostankov³⁷, A.Ouraou³⁴, M.Paganoni²⁵, R.Pain²⁰, H.Palka²⁷,
 T.Papadopoulou²⁸, L.Pape⁷, A.Passeri³⁵, M.Pegoraro³¹, J.Pennanen¹², V.Perevoschikov³⁷, M.Pernicka⁴³,
 A.Perrotta⁵, F.Pierre³⁴, M.Pimenta¹⁸, O.Pingot², M.E.Pol⁷, G.Polok¹⁵, P.Poropat⁴⁰, P.Privitera¹⁴, A.Pullia²⁵,
 D.Radojicic³⁰, S.Ragassi²⁵, P.N.Ratoff¹⁷, A.L.Read²⁹, N.G.Redaeli²⁵, M.Regler⁴³, D.Reid¹⁹, P.B.Renton³⁰,
 L.K.Resvanis³, F.Richard¹⁶, M.Richardson¹⁹, J.Ridky¹³, G.Rinaudo³⁹, I.Roditi⁷, A.Romero³⁹, I.Roncagliolo¹⁰,
 P.Ronchese³¹, V.Ronjin³⁷, C.Ronnqvist¹², E.I.Rosenberg¹, U.Rossi⁵, E.Rosso⁷, P.Roudeau¹⁶, T.Rovelli⁵,
 W.Ruckstuhl²⁷, V.Ruhlmann³⁴, A.Ruis³⁸, K.Rybicki¹⁵, H.Saarikko¹², Y.Sacquin³⁴, G.Sajot¹¹, J.Salt⁴²,
 E.Sanchez⁴², J.Sanchez²³, M.Sannino¹⁰, M.Schaeffer⁸, S.Schael¹⁴, H.Schneider¹⁴, M.A.E.Schyns⁷, F.Scuri⁴⁰,
 A.M.Segar³⁰, R.Sekulin³², M.Sessa⁴⁰, G.Sette¹⁰, R.Seufert¹⁴, R.C.Shellard⁷, P.Siegrist³⁴, S.Simonetti¹⁰,
 F.Simonetto³¹, A.N.Sissakian¹³, T.B.Skaali²⁹, G.Skjevling²⁹, G.Smadja^{34,22}, G.R.Smith³², R.Sosnowski⁴⁴,

T.S.Spaso¹¹, E.Spiriti³⁵, S.Squarcia¹⁰, H.Staek⁴⁵, C.Stanescu³⁵, G.Stavropoulos⁹, F.Stichelbaut², A.Stocchi¹⁶, J.Strauss⁴³, R.Strub⁸, M.Szczekowski⁴⁴, M.Szeptycka⁴⁴, P.Szymanski⁴⁴, T.Tabarelli²⁵, S.Tavernier², G.E.Theodosiou⁹, A.Tilquin²⁴, J.Timmermans²⁷, V.G.Timofeev¹³, L.G.Tkatchev¹³, T.Todorov¹³, D.Z.Toet²⁷, O.Toker¹², E.Torassa³⁹, L.Tortora³⁵, M.T.Trainor³⁰, D.Treille⁷, U.Trevisan¹⁰, W.Trischuk⁷, G.Tristram⁶, C.Troncon²⁵, A.Tsirou⁷, E.N.Tsyganov¹³, M.Turala¹⁵, R.Turchetta⁸, M-L.Turluer³⁴, T.Tuuva¹², I.A.Tyapkin¹³, M.Tyndel³², S.Tzaniaris⁷, B.Ueberschaer⁴⁵, S.Ueberschaer⁴⁵, O.Ullaland⁷, V.Uvarov³⁷, G.Valenti⁵, E.Vallazza³⁹, J.A.Valls Ferrer⁴², C.Vander Velde², G.W.Van Apeldoorn²⁷, P.Van Dam²⁷, W.K.Van Doninck², J.Varela¹⁸, P.Vas⁷, G.Vegni²⁵, L.Ventura³¹, W.Venus³², F.Verbeure², L.S.Vertogradov¹³, L.Vibert²⁰, D.Vilanova³⁴, N.Vishnevsky³⁷, L.Vitale⁴⁰, E.Vlasov³⁷, S.Vlassopoulos²⁸, A.S.Vodopyanov¹³, M.Vollmer⁴⁵, S.Volponi⁵, G.Voulgaris³, M.Voutilainen¹², V.Vrba³⁵, H.Wahlen⁴⁵, C.Walck³⁸, F.Waldner⁴⁰, M.Wayne¹, P.Weilhammer⁷, J.Werner⁴⁵, A.M.Wetherell⁷, J.H.Wickens², J.Wikne²⁹, G.R.Wilkinson³⁰, W.S.C.Williams³⁰, M.Winter⁸, D.Wormald²⁹, G.Wormser¹⁶, K.Woschnagg⁴¹, N.Yamdagni³⁸, P.Yepes⁷, A.Zaitsev³⁷, A.Zalewska¹⁵, P.Zalewski¹⁶, D.Zavrtanik⁷, E.Zevgolatakos⁹, G.Zhang⁴⁵, N.I.Zimin¹³, M.Zito³⁴, R.Zitoun²⁰, R.Zukanovich Funchal⁶, G.Zumerle³¹, J.Zuniga⁴²

¹ Ames Laboratory and Department of Physics, Iowa State University, Ames IA 50011, USA

² Physics Department, Univ. Instelling Antwerpen, Universiteitsplein 1, B-2610 Wilrijk, Belgium and IIHE, ULB-VUB, Pleinlaan 2, B-1050 Brussels, Belgium and Service de Phys. des Part. Elém., Faculté des Sciences, Université de l'Etat Mons, Av. Maistriau 19, B-7000 Mons, Belgium

³ Physics Laboratory, University of Athens, Solonos Str. 104, GR-10680 Athens, Greece

⁴ Department of Physics, University of Bergen, Allégaten 55, N-5007 Bergen, Norway

⁵ Dipartimento di Fisica, Università di Bologna and INFN, Via Irnerio 46, I-40126 Bologna, Italy

⁶ Collège de France, Lab. de Physique Corpusculaire, 11 pl. M. Berthelot, F-75231 Paris Cedex 05, France

⁷ CERN, CH-1211 Geneva 23, Switzerland

⁸ Division des Hautes Energies, CRN - Groupe DELPHI and LEPsi, B.P.20 CRO, F-67037 Strasbourg Cedex, France

⁹ Institute of Nuclear Physics, N.C.S.R. Demokritos, P.O. Box 60228, GR-15310 Athens, Greece

¹⁰ Dipartimento di Fisica, Università di Genova and INFN, Via Dodecaneso 33, I-16146 Genova, Italy

¹¹ Institut des Sciences Nucléaires, Université de Grenoble 1, F-38026 Grenoble, France

¹² Research Institute for High Energy Physics, University of Helsinki, Siltavuorenpenger 20 C, SF-00170 Helsinki 17, Finland

¹³ Joint Institute for Nuclear Research, Dubna, Head Post Office, P.O. Box 79, 101 000 Moscow, USSR.

¹⁴ Institut für Experimentelle Kernphysik, Universität Karlsruhe, Postfach 6980, D-7500 Karlsruhe 1, FRG

¹⁵ High Energy Physics Laboratory, Institute of Nuclear Physics, Ul. Kawiora 26 a, PL-30055 Krakow 30, Poland

¹⁶ Université de Paris-Sud, Lab. de l'Accélérateur Linéaire, Bat 200, F-91405 Orsay, France

¹⁷ School of Physics and Materials, University of Lancaster - Lancaster LA1 4YB, UK

¹⁸ LIP, Av. Elias Garcia 14 - 1e, P-1000 Lisbon Codex, Portugal

¹⁹ Department of Physics, University of Liverpool, P.O. Box 147, GB - Liverpool L69 3BX, UK

²⁰ LPNHE, Universités Paris VI et VII, Tour 33 (RdC), 4 place Jussieu, F-75230 Paris Cedex 05, France

²¹ Department of Physics, University of Lund, Sölvegatan 14, S-22363 Lund, Sweden

²² Université Claude Bernard de Lyon, 43 Bd du 11 Novembre 1918, F-69622 Villeurbanne Cedex, France

²³ Universidad Complutense, Avda. Complutense s/n, E-28040 Madrid, Spain

²⁴ Univ. d'Aix - Marseille II - Case 907 - 70, route Léon Lachamp, F-13288 Marseille Cedex 09, France

²⁵ Dipartimento di Fisica, Università di Milano and INFN, Via Celoria 16, I-20133 Milan, Italy

²⁶ Niels Bohr Institute, Blegdamsvej 17, DK-2100 Copenhagen 0, Denmark

²⁷ NIKHEF-H, Postbus 41882, NL-1009 DB Amsterdam, The Netherlands

²⁸ National Technical University, Physics Department, Zografou Campus, GR-15773 Athens, Greece

²⁹ Physics Department, University of Oslo, Blindern, N-1000 Oslo 3, Norway

³⁰ Nuclear Physics Laboratory, University of Oxford, Keble Road, GB - Oxford OX1 3RH, UK

³¹ Dipartimento di Fisica, Università di Padova and INFN, Via Marzolo 8, I-35131 Padua, Italy

³² Rutherford Appleton Laboratory, Chilton, GB - Didcot OX11 0QX, UK

³³ Dipartimento di Fisica, Università di Roma II and INFN, Tor Vergata, I-00173 Rome, Italy

³⁴ CEN-Saclay, DPhPE, F-91191 Gif-sur-Yvette Cedex, France

³⁵ Istituto Superiore di Sanità, Ist. Naz. di Fisica Nucl. (INFN), Viale Regina Elena 299, I-00161 Rome, Italy

³⁶ Facultad de Ciencias, Universidad de Santander, av. de los Castros, E - 39005 Santander, Spain

³⁷ Inst. for High Energy Physics, Serpukov P.O. Box 35, Protvino, (Moscow Region), USSR.

³⁸ Institute of Physics, University of Stockholm, Vanadisvägen 9, S-113 46 Stockholm, Sweden

³⁹ Dipartimento di Fisica Sperimentale, Università di Torino and INFN, Via P. Giuria 1, I-10125 Turin, Italy

⁴⁰ Dipartimento di Fisica, Università di Trieste and INFN, Via A. Valerio 2, I-34127 Trieste, Italy

and Istituto di Fisica, Università di Udine, I-33100 Udine, Italy

⁴¹ Department of Radiation Sciences, University of Uppsala, P.O. Box 535, S-751 21 Uppsala, Sweden

⁴² Inst. de Fisica Corpuscular IFIC, Centro Mixto Univ. de Valencia-CSIC, and Departamento de Fisica Atomica Molecular y Nuclear, Univ. de Valencia, Avda. Dr. Moliner 50, E-46100 Burjassot (Valencia), Spain

⁴³ Institut für Hochenergiephysik, Österreichisch Akad. d. Wissensch., Nikolsdorfergasse 18, A-1050 Vienna, Austria

⁴⁴ Inst. Nuclear Studies and, University of Warsaw, Ul. Hoza 69, PL-00681 Warsaw, Poland

⁴⁵ Fachbereich Physik, University of Wuppertal, Postfach 100 127, D-5600 Wuppertal 1, FRG

1 Introduction

Experiments at proton-(anti)proton colliders [1] have shown that starting from roughly the highest ISR energy, $\sqrt{s} = 60$ GeV, the mean transverse momentum $\langle p_t \rangle$ increases with the number of charged particles n_{ch} produced in the collision and the effect becomes more pronounced as the collision energy increases. Several explanations of this observation have been proposed in different pictures of hadronic collisions [2]. The phenomenon, however, is not fully understood and the subject requires further study. In particular, a comparison of data coming from different types of collisions should provide additional tests of the models.

Recently it was pointed out that in certain models the observation of the multiplicity dependence of $\langle p_t \rangle$ in hadronic collisions leads to a very natural expectation of a similar phenomenon in e^+e^- annihilations at high energies [3]. The good understanding of hadronic production in e^+e^- annihilations in terms of "QCD inspired" Monte Carlo models [4],[5] allows detailed tests of the origin of the phenomenon.

In this paper we present the first experimental results for the dependence of $\langle p_t \rangle$ on charged particle multiplicity in high energy e^+e^- annihilations using the DELPHI detector and compare them with the JETSET 7.2 Lund Monte Carlo model. The data selection and the data correction procedures are described in section 2 and 3, respectively. The results for $\langle p_t \rangle$ and n_{ch} correlations are presented in section 4. The summary and conclusions are given in section 5.

2 Data Selection

The data were recorded with the DELPHI detector at the CERN e^+e^- collider LEP in 1990. The detector, the trigger conditions and the readout system are described in detail in ref. [6]. Here we summarize only the specific properties relevant to the following analysis.

The tracks of charged particles were measured in the Time Projection Chamber (TPC) and in the Inner and Outer Detectors. Up to 16 space points in the TPC were used for track reconstruction by the DELPHI analysis package, DELANA [7]. The average momentum resolution was found to be $\delta p/p^2 = \pm 0.0012$ (GeV/c) $^{-1}$. Points on neighbouring tracks could be distinguished if they were separated by at least 15 mm in z , the coordinate along the beam axis, and in $r\phi$, the azimuthal coordinate. No significant differences in track-finding efficiency were observed between the data and the Monte Carlo simulation.

The tracks of charged particles were retained if:

- (a) they extrapolated back to within 5 cm of the beam axis in r and to within 10 cm of the nominal crossing point in z ,
- (b) the particle momentum, p , was larger than 0.1 GeV/c,
- (c) their measured length was greater than 50 cm,
- (d) their polar angle was between 25° and 155° .

Hadronic events were then selected by requiring that:

- (a) the total energy of charged particles $E_{ch} = \sum_i E_i$ in each of the two hemispheres defined with respect to the beam axis exceeded 3 GeV, where E_i were the particles' energies (assuming the pion mass),

(b) the total energy of charged particles seen in both hemispheres together exceeded 15 GeV,

(c) there were at least 5 charged particles with momenta above 0.2 GeV/c,

(d) the polar angle, θ , of the sphericity axis was in the range $50^\circ < \theta < 130^\circ$.

The last cut ensured that the retained events were well contained inside the TPC. The resulting data sample comprised 80521 events. The last cut ensured that the retained events were well contained inside the TPC. After all four cuts, events due to beam-gas scattering and to $\gamma\gamma$ interactions were reduced to below 0.1 % of the sample. The largest background was due to $\tau^+\tau^-$ events. From Monte Carlo simulation this was calculated to be 0.15 % of the sample. Since this background influences mainly events with $n_{ch} = 6$ in our sample, in the following we will consider only events with $n_{ch} > 6$.

3 Data Correction Procedure

Monte Carlo simulations were used to correct the distributions for the geometrical acceptance and kinematical cuts, the detector resolution, acceptance inefficiencies, particle interactions in the material of the detector, other detector imperfections and the effects of radiated photons. The Lund parton-shower model (JETSET 7.2) was used to generate 74485 Z^0 events decaying to pairs of u,d,c,s and b quarks. A correction factor $C(x)$ for each bin in each data plot was then obtained by comparing the bin occupancy at the beginning of the simulation (the "true" distribution) with the bin occupancy after reconstruction and selection (the "observed" distribution):

$$C(x) = \left(\frac{1}{N} \frac{dn}{dx} \right)_{\text{true}} / \left(\frac{1}{N} \frac{dn}{dx} \right)_{\text{observed}}$$

The "true" distributions were constructed from the final state particles of lifetime above 10^{-9} s in events generated without initial state radiation that had not yet been tracked through the detector. The "observed" distributions were constructed from the final state particles observed after tracking events generated with initial state radiation through the DELPHI detector to produce simulated raw data which were then processed through the same reconstruction and analysis programs as the real data. The value of the correction factor $C(x)$ lies between 0.8 and 1.1 for all the data points. This factor was used to correct the experimental data.

4 Results on Multiplicity Dependence of Mean Transverse Momenta

The dependence on charged particle multiplicity of the mean transverse momenta will be studied both in the event plane - $\langle p_{t,in} \rangle$ and in the direction perpendicular to the event plane - $\langle p_{t,out} \rangle$. Both directions are defined in the standard way using the second rank tensor constructed from the final charged hadron momenta [8]. The sphericity axis is used as the longitudinal axis of the event.

The dependence of $\langle p_{t,in} \rangle$ and $\langle p_{t,out} \rangle$ on charged particle multiplicities in e^+e^- annihilations at $\sqrt{s} = 91$ GeV is shown in figs. 1 a and 1 b, respectively. A strong

correlation of the mean transverse momenta with n_{ch} can be observed: $\langle p_{t,in} \rangle$ increases by about 50 % from $n_{ch} = 8$ to $n_{ch} = 30$ and then flattens out at higher multiplicities. A similar behaviour is observed for $\langle p_{t,out} \rangle$ but the flattening at high multiplicities is here not visible. Although the absolute $\langle p_{t,out} \rangle$ values are smaller than $\langle p_{t,in} \rangle$, the relative increase is roughly the same. Both correlations are well reproduced by JETSET 7.2 Lund Parton Shower model [4], although the data for $\langle p_{t,in} \rangle$ show slightly smaller dependence on n_{ch} than the model. This small discrepancy is consistent with our earlier observation that the increase in total $\langle p_{t,in} \rangle$ with energy is smaller in the data than in the Monte Carlo models [8].

In figs. 2 a and 2 b, respectively, the correlations of $\langle p_{t,in} \rangle$ and $\langle p_{t,out} \rangle$ with n_{ch} are shown for different rapidity intervals. The main contribution to the strong increase of $\langle p_{t,in} \rangle$ with n_{ch} comes from particles in the central rapidity region. For particles with $|y| > 2.0$ the increase of $\langle p_{t,in} \rangle$ is less steep and for the still higher rapidity region $|y| > 3.0$ there is almost no dependence on n_{ch} , except a slightly negative correlation for large multiplicities. Some flattening of the $\langle p_{t,out} \rangle$ distributions for faster particles is also observed, but here the dependence of the effect on the rapidity interval is smaller. These trends are well described by the Lund Parton Shower model.

Two mechanisms in high energy e^+e^- annihilations could lead to a positive correlation of $\langle p_t \rangle$ with n_{ch} : heavy quark production and gluon radiation. The comparison of the events generated by the Lund Monte Carlo for the sample with beauty quark pairs removed from the generation with the sample of all flavours events shows that the contribution from production of heavy quark pairs to the increase of $\langle p_{t,in} \rangle$ and $\langle p_{t,out} \rangle$ with multiplicity is negligible [3].

The agreement of the Lund Parton Shower model with the data suggests that the main mechanism responsible for these correlations is gluon radiation. To test this assertion in our data, we use events with a specific number of jets, $N_{JET} = 2, 3, 4$, defined by the JADE cluster finding algorithm described in detail in ref. [9]. The scaled pair mass of particles i and j from two resolvable jets, $y_{ij} = M_{ij}^2/s$ was required to exceed a threshold value $y_{CUT} = 0.03$. Particles with $y_{ij} < y_{CUT}$ are combined into a single cluster. The jet multiplicity is the number of clusters determined by the jet finding algorithm.

The correlations of mean transverse momenta with n_{ch} are shown in figs. 3 a and 3 b for the separate classes. The mean transverse momenta increase with the number of jets, but for a given number of jets there is only a relatively weak dependence of $\langle p_{t,in} \rangle$ and $\langle p_{t,out} \rangle$ on n_{ch} . This means that the observed correlation for the full sample arises mainly from the mixing of different classes of events. The energy dependence of the correlations of $\langle p_t \rangle$ with n_{ch} could then be understood in terms of the increased fraction of events with a larger number of jets at higher energies. The observed behaviour is well reproduced by the Lund Parton Shower model, where the events with 3 and 4 jets may be attributed to quark - antiquark production with additional gluon radiation.

An interesting pattern can be observed in figs. 3 a and 3 b. The direction of the hardest gluon radiation usually defines the event plane and therefore the most energetic gluon contributes mainly to $\langle p_{t,in} \rangle$, causing the large difference between the values of $\langle p_{t,in} \rangle$ for 2-jet and 3-jet samples.

The next, softer gluon, is frequently radiated out of the event plane, and provides a smaller contribution to $\langle p_{t,in} \rangle$, as is illustrated by the difference between the 3- and the 4-jet samples in fig. 3 a. The opposite behaviour can be observed for $\langle p_{t,out} \rangle$. Here the main contribution arises from the second, softer gluon, causing the large difference between the values of $\langle p_{t,out} \rangle$ for 3- and 4-jet samples, while the smaller contribution

from the more energetic gluon can be observed in the difference between the values of $\langle p_{t,out} \rangle$ for 2- and 3-jet events.

The choice of y_{CUT} defines the resolution for the observation of jets. With larger y_{CUT} (worse resolution) softer jets will not be resolved and the event will be classified in a sample with a smaller number of jets. The number of events in the 2-jet sample will increase and these events will include more energetic gluon radiation. In the limit with a very large y_{CUT} all the events will be classified in the "2-jet" sample and the correlations for this sample will reproduce the correlations observed for the total sample. The correlations of mean p_t and n_{ch} for the samples with the specific number of jets should therefore depend on the jet definition and the choice of y_{CUT} . To study this dependence $\langle p_{t,in} \rangle$ and $\langle p_{t,out} \rangle$ are plotted in figs. 4 a and 4 b as a function of n_{ch} for 2-jet samples of events classified with different y_{CUT} parameters. The correlations increase for the samples with a larger y_{CUT} both for $\langle p_{t,in} \rangle$ and $\langle p_{t,out} \rangle$. They are even slightly negative for $\langle p_{t,in} \rangle$ in the sample with the very low $y_{CUT} = 0.01$.

A somewhat different behaviour can be observed for the 3-jet samples shown in figs. 5 a and 5 b. With increasing y_{CUT} some events are shifted from the 4-jet class to the 3-jet class, similarly as in the case of the 2-jet sample discussed above, but in addition some events are removed from the 3-jet class to the 2-jet class. These two effects are reflected in the more complicated dependence of the correlations in the 3-jet sample on y_{CUT} . The correlations for $\langle p_{t,in} \rangle$ are slightly positive and similar for $y_{CUT} = 0.01$ and for $y_{CUT} = 0.03$, but strongly negative for the larger value, $y_{CUT} = 0.10$. The correlations for $\langle p_{t,out} \rangle$ increase only slightly with increasing y_{CUT} .

For all the samples the values of $\langle p_{t,in} \rangle$ and $\langle p_{t,out} \rangle$ increase with increasing y_{CUT} .

All the trends in the data for different y_{CUT} samples are well described by the Lund Parton Shower model. There are, however, small but significant differences between the experimental results and the model predictions in almost all the samples.

5 Summary and Conclusions

We have presented the first results showing large positive correlations of mean transverse momenta $\langle p_{t,in} \rangle$ and $\langle p_{t,out} \rangle$ and charged particle multiplicity in high energy e^+e^- annihilations. The effect is well described by the Lund Parton Shower model, where it arises from gluon radiation off highly virtual quarks. There are, however, small but significant differences between the experimental results and the model predictions. Some of the properties of the correlations, like the rapidity dependence or the flattening of $\langle p_t \rangle$ at high multiplicities, are similar to those observed in high energy hadronic reactions [1].

The correlations of $\langle p_t \rangle$ and n_{ch} observed in our data for e^+e^- annihilations at high energy can provide an additional test of models for multiparticle production both in e^+e^- and in hadron-hadron collisions.

Acknowledgements

We are greatly indebted to our technical collaborators and to the funding agencies for their support in building and operating the DELPHI detector, and to the members of the CERN-SL Division for the excellent performance of the LEP collider.

References

- [1] A.Breakstone et al. (SFM), Phys. Lett. B132, 463 (1983); Z. Phys. C33, 333 (1987); Phys. Lett. B183, 227 (1987); Europhys. Lett. 7, 131 (1988); W.Bell et al., Z. Phys. C27, 191 (1985); G.Arnison et al. (UA1), Phys. Lett. B118, 167 (1982); R.E.Ansorge et al. (UA5), Z. Phys. C41, 179 (1988); T.Alexopoulos et al. (E735), Phys. Rev. Lett. 60, 1622 (1988); T.H.Burnett et al. (JACEE), Phys. Rev. Lett. 57, 3249 (1986).
- [2] S.Barshay, Phys. Lett. B127, 129 and Phys. Rev. D29, 1010 (1984); A.Capella and A.Krzywicki, Phys. Rev. D29, 1007 (1984); A.Capella, J.Tran Thanh Van and J.Kwiecinski, Phys. Rev. Lett. 58, 2015 (1987); F.W.Bopp, P.Aurenche and J.Ranft, Phys. Rev. D33, 1867 (1986); E.V.Shuryak, Phys. Rep. 61, 71 (1980); L.Van Hove, Phys. Lett. B118, 138 (1982); M.Kataja et al., Phys. Rev. D34, 2755 (1986); X.Wang and R.C.Hwa, Phys. Rev. D39, 187 (1989); G.Pancheri and Y.N.Srivastava, Phys. Lett. B159, 69 (1985); T.Sjostrand and M.van Zijl, Phys. Rev. D36, 2019 (1987); A.D.Martin and C.J.Maxwell, Z. Phys. C34, 71 (1987); T.K.Gaisser and T.Stanev, Phys. Lett. B129, 375 (1989).
- [3] M.Szczekowski and G.Wilk, Phys. Rev. D44, R577 (1991).
- [4] M.Bengtsson and T.Sjostrand, Phys. Lett. B185, 435 (1987).
- [5] G.Marchesini and B.R.Webber, Nucl. Phys. B238, 1 (1984).
- [6] P.Aarnio et al. (DELPHI), Nucl. Instr. Methods A303, 233 (1991).
- [7] DELPHI Data Analysis Program - User's Guide $\text{DELPHI} = \text{W} = \text{1} (1989)$, unpublished.
- [8] P.Aarnio et al. (DELPHI), Phys. Lett. B240,
- [9] W.Bartel et al. (JADE), Z. Phys. C33, 23 (1988).

Figure Captions

- Fig.1 Dependence of mean transverse momenta in the event plane - $\langle p_{t,in} \rangle$ (a) and in the direction perpendicular to the event plane - $\langle p_{t,out} \rangle$ (b) on charged particle multiplicity in e^+e^- annihilations into hadrons at $\sqrt{s} = 91$ GeV. The data are compared with the predictions of the Lund Parton Shower model.
- Fig.2 Dependence, (a) of $\langle p_{t,in} \rangle$, (b) of $\langle p_{t,out} \rangle$, on n_{ch} , shown for three regions of rapidity: a central region $|y| < 2.0$ and two outer regions $|y| > 2.0$ and $|y| > 3.0$. The data are compared with the predictions of the Lund Parton Shower model.
- Fig.3 Dependence, (a) of $\langle p_{t,in} \rangle$, (b) of $\langle p_{t,out} \rangle$, on n_{ch} , shown for events with different numbers of jets, $N_{JET} = 2, 3, 4$. The data are compared with the predictions of the Lund Parton Shower model.
- Fig.4 Dependence, (a) of $\langle p_{t,in} \rangle$, (b) of $\langle p_{t,out} \rangle$, on n_{ch} , shown for events in 2-jet samples defined with different choices of the y_{CUT} parameter: $y_{CUT} = 0.01, 0.03, 0.10$. The data are compared with the predictions of the Lund Parton Shower model.
- Fig.5 Dependence, (a) of $\langle p_{t,in} \rangle$, (b) of $\langle p_{t,out} \rangle$, on n_{ch} , shown for events in 3-jet samples defined with different choices of the y_{CUT} parameter: $y_{CUT} = 0.01, 0.03, 0.10$. The data are compared with the predictions of the Lund Parton Shower model.

Figure 1 a

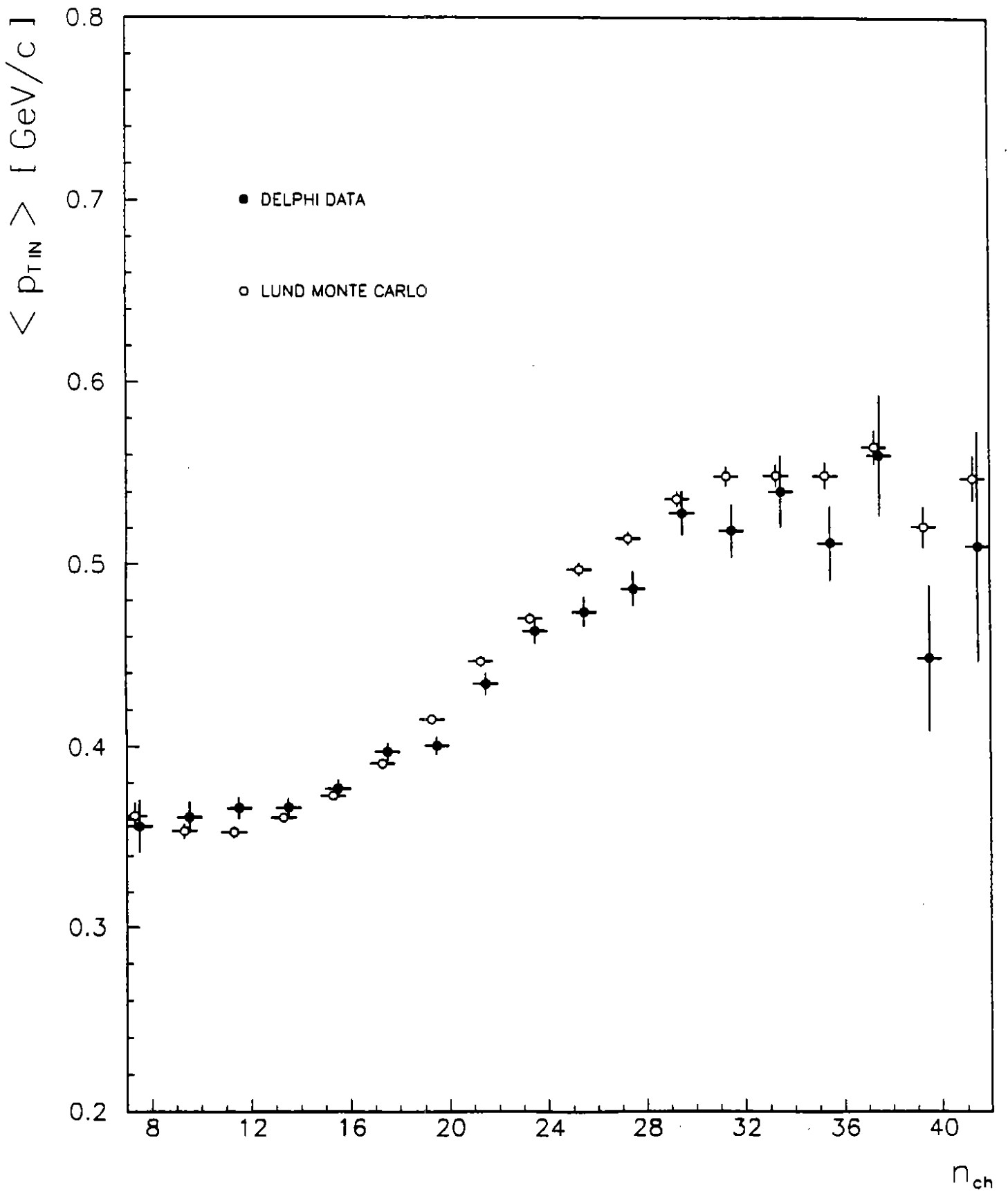


Figure 1 b

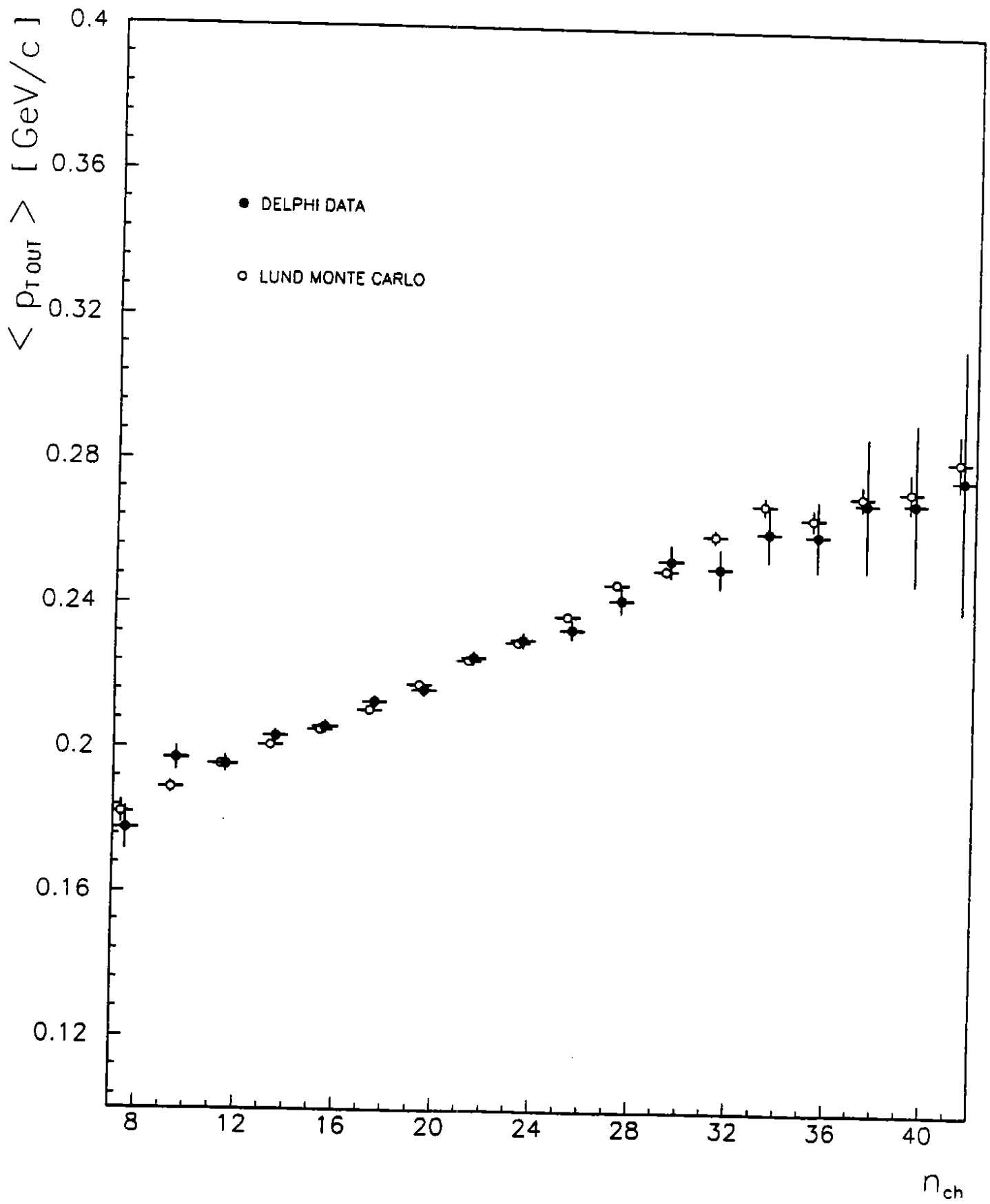


Figure 2 a

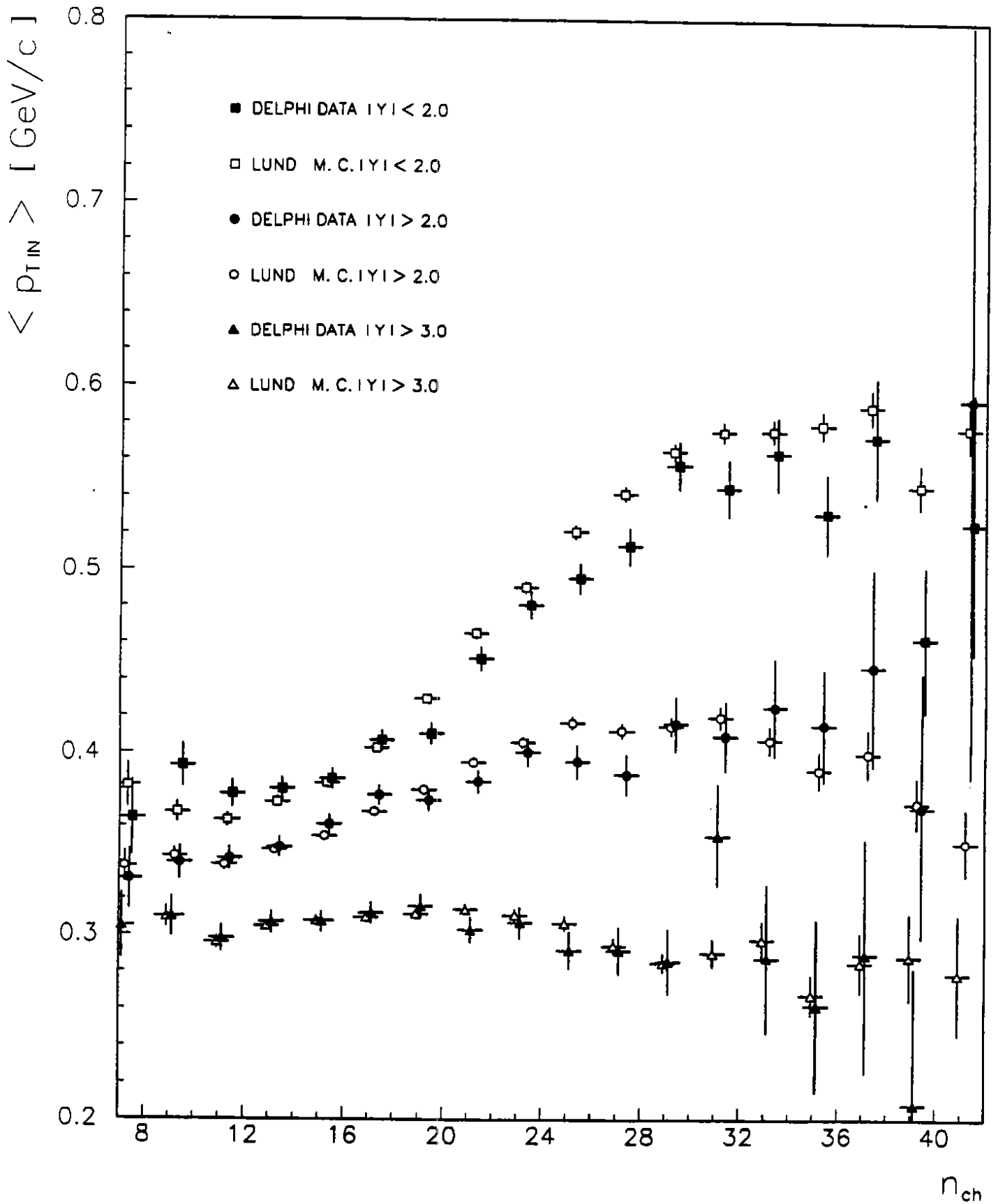


Figure 2 b

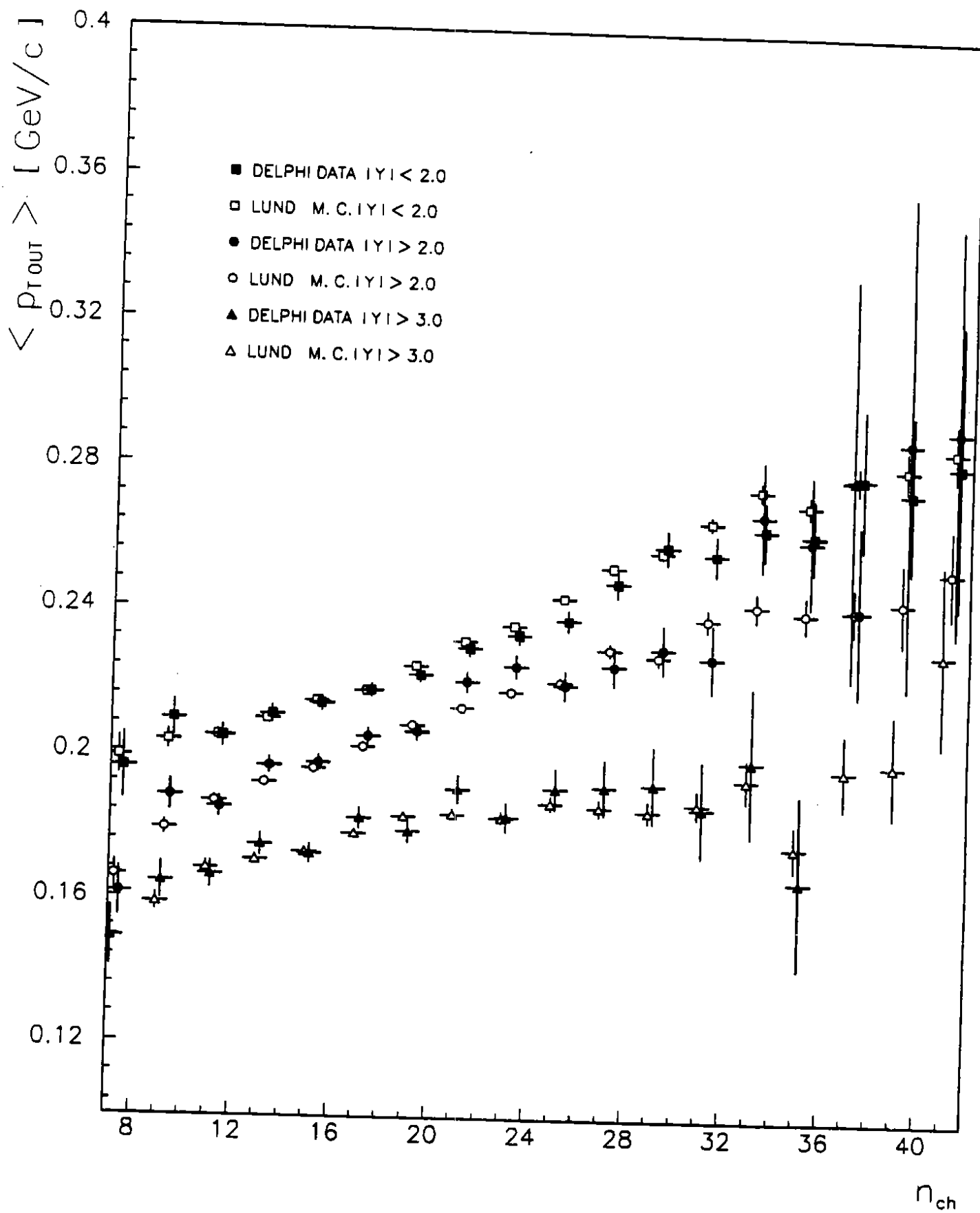


Figure 3 a

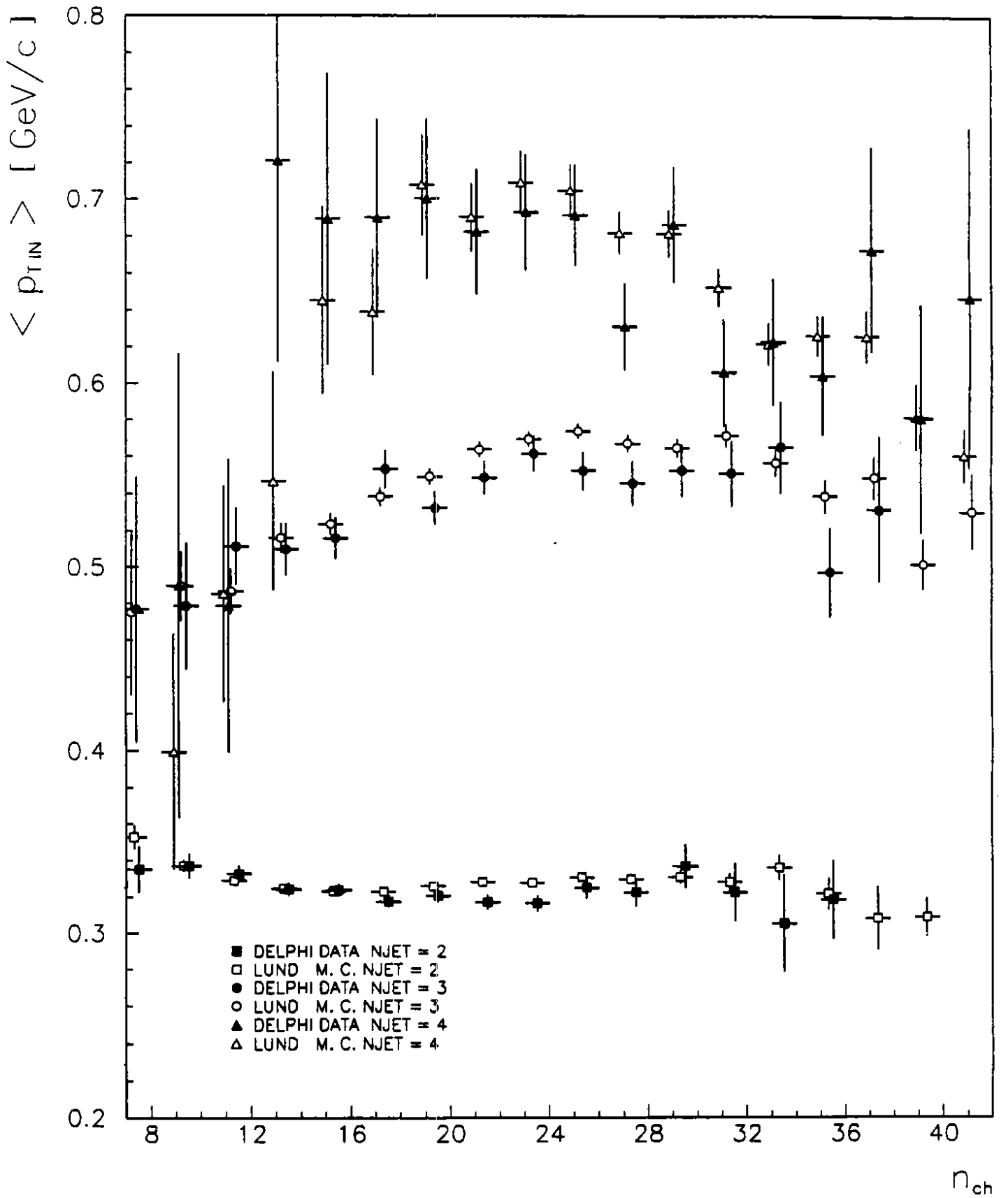


Figure 3 b

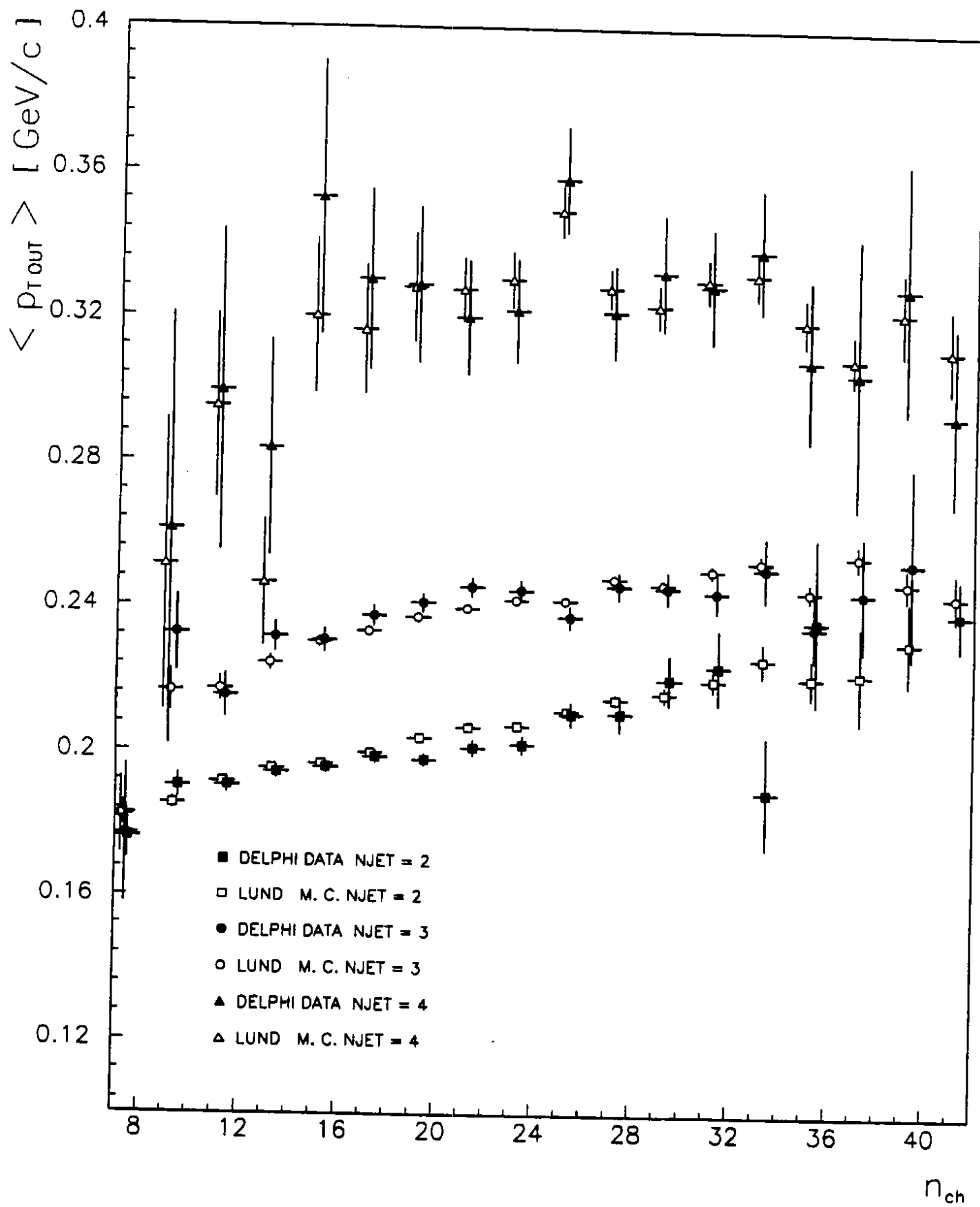


Figure 4 a

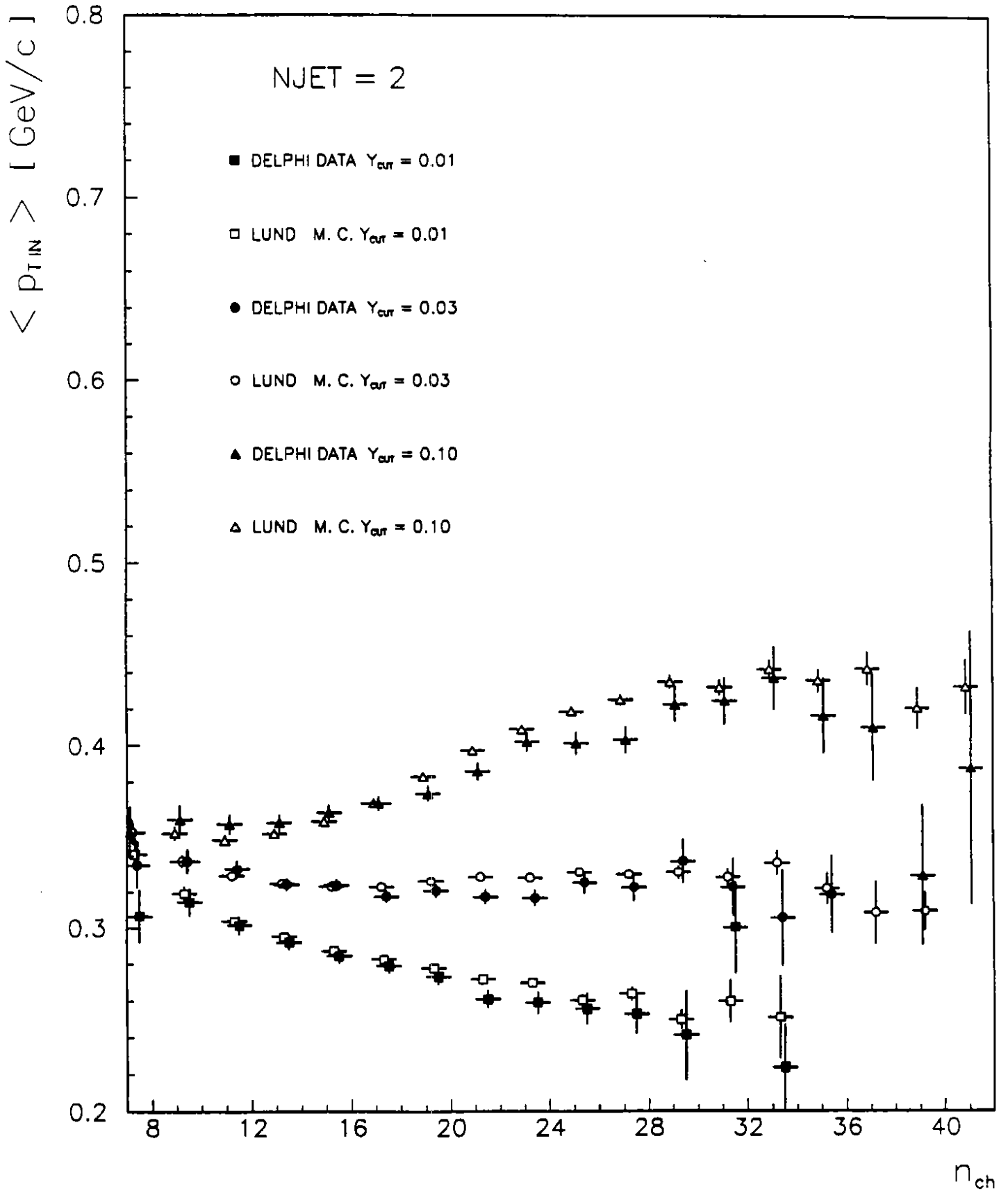


Figure 4 b

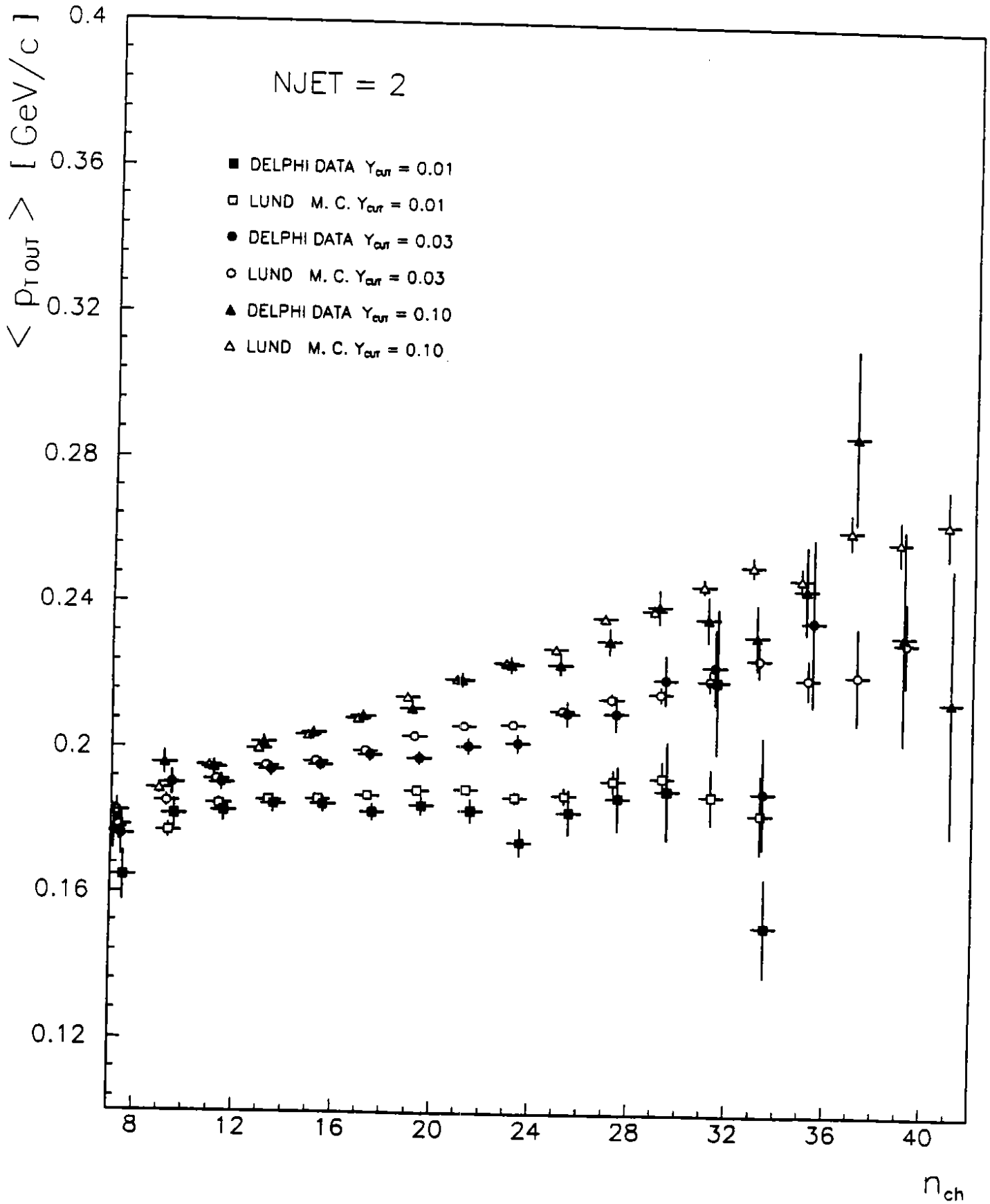


Figure 5 a

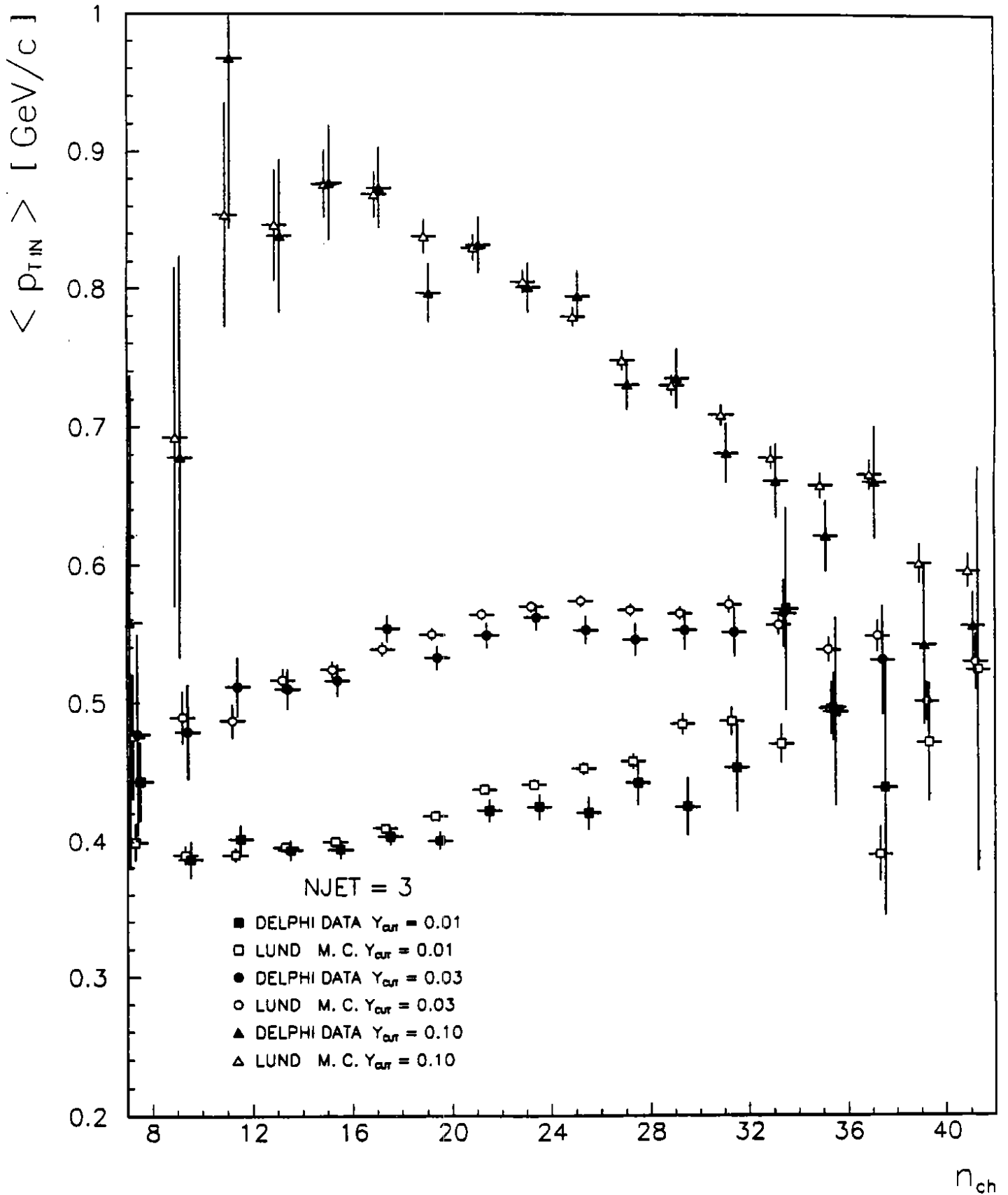


Figure 5 b

